Journal of Applied Polymer Science

Aging of polyamide 11. Part 3: Multiscale model predicting the mechanical properties after hydrolytic degradation

Tobiasz Mazan,[1] Jens Kjær Jørgensen,[2] Andreas Echtermeyer[1]
[1]Department of Engineering Design and Materials, Norwegian University of Science and Technology, Trondheim 7491, Norway
[2]SINTEF Materials and Chemistry, Oslo 0314, Norway
Correspondence to: T. Mazan (E-mail: tobiasz.mazan@ntnu.no)

ABSTRACT: A holistic general multiscale model of polymer degradation has been applied to predict the mechanical properties of polyamide 11 after the hydrolytic ageing. Results for elastic modulus, tensile strength, and embrittlement threshold have been compared with experimental aging in deoxygenated water at 120°C. For all studied properties the modeled trend is close to the experimental test results confirming hydrolysis induced chain scission and chemicrystalization as the two main mechanisms of property change. This suggests that the multiscale modeling methodology can provide a valuable alternative to accelerated aging tests. The model also indicated that the crystalline phase does play a role in the plastic deformation. Moreover, the mechanical equilibrium between effects of macromolecule degradation and an increased degree of crystallinity has been described. © 2015 Wiley Periodicals, Inc. J. Appl. Polym. Sci. **2015**, *132*, 42792.

KEYWORDS: degradation; mechanical properties; oil and gas; polyamides; theory and modeling

Received 30 March 2015; accepted 30 July 2015
DOI: 10.1002/app.42792

INTRODUCTION

Polyamide 11 (PA11) is commonly used as a material for the internal pressure sheaths in offshore flexible risers.[1] It possesses good mechanical and barrier properties; however, it is also known to undergo chemical degradation once exposed to oil field exploration environments, especially water.[2]

Therefore, long-term performance of the riser under chemical and mechanical factors must be evaluated.[3] As of today, long-term performance is evaluated by simple extrapolation of the experimental data for a certain material (here PA11) in the expected environment to lifetimes up to 50 years. No consideration is given to the actual mechanisms behind the degradation process.[4]

Despite extensive laboratory testing; which requires labor, time and resources; actual failure in the field often happens long before (or after) the expected one. Also, without scientific understanding of the processes in the microscale, extrapolation of the results to different application cases is very difficult. In order to improve cost, accuracy, and generality of predictions a general model of degradation is proposed here.

The present article as Part 3 of a series describes the model considering the mechanical properties as a function of previously obtained morphology predictions. This aspect was presented in Part 2 along with the details of the general modeling methodology proposed.[5] The experiments were presented in Part 1.[6]

Multiscale Model of Degradation

The multiscale approach is presented here as a way to improve the long-term property evaluations. Many models operating on individual stages of the proposed method exist already. Nevertheless so far the problem has not been treated holistically to form a multiscale model of degradation from the single-scale models. The purpose of this study is to change the state of the art in this research area by linking microscopic degradation induced by chemical factors to macroscale properties of the polymer.

Details of the model both in the general case and as applied to PA11 were presented in the Part 2 of the series.[5] The following section provides a short summary of this description. The input and output parameters of all constituent models used here for PA11 are also presented later in the article. The multiscale model proposed here consists of four fundamental stages as described below.

Stage 1: Concentration Profile. The concentration profile of the environmental agents (water, oxygen, acids, etc.) in the polymer must be evaluated with time. Normally Fick's diffusion characteristic is assumed; however, if the shape of the

concentration profiles is of key importance the validity of this assumption should be checked.

Diffusion in polyamides is usually considered to follow Fick's law.[7] The diffusion coefficient of water in Polyamide 11 was taken from the literature.[7] Its value shows, that for PA11 aged in water diffusion proceeds very fast.[1,7] Therefore the environmental agent is uniformly distributed within the material. Polyamide 11 will be here considered to be completely saturated, thus Stage 1 will not be considered in the later parts of the article. It is assumed that the amorphous part will absorb water while the crystalline part remains mostly unaffected.

Stage 2: Kinetic Model—Molecular Level. The effect of chemical action of the environmental agent on the polymer molecular properties with time must be found. This is a key part of the methodology as it predicts the molecular response in the long-term perspective for which direct empirical evaluation would be impractical or impossible. The most important property changes addressed in this task are the molecular weight decrease of the amorphous phase and the degree of crystallinity increase.[5,6]

Jacques kinetic model was chosen to calculate the kinetics of hydrolytic chain-scission due to its confirmed accuracy and relative simplicity.[8] Chain scissions result in decreased molecular weight, which in turn decreases stiffness in the amorphous phase and will eventually cause the embrittlement of the entire material.[9]

The molecular weight evolution in Jacques kinetic model is governed by the following equation:[8]

$$M_n(t)=M_{\mathrm{ne}}\frac{M_{n0}^{-1}+M_{\mathrm{ne}}^{-1}+\left(M_{\mathrm{ne}}^{-1}-M_{n0}^{-1}\right)\exp\left(-Kt\right)}{M_{n0}^{-1}+M_{\mathrm{ne}}^{-1}-\left(M_{\mathrm{ne}}^{-1}-M_{n0}^{-1}\right)\exp\left(-Kt\right)} \quad (1)$$

where M_{ne}—equilibrium molecular mass; M_{n0}—initial molecular mass; K—experimental pseudo rate constant.

The Jacques kinetic model was presented in more detail in a previous article[5] of the series as well as in the original reference.[8]

Moreover the chain scissions tend to destroy the entanglement network in the amorphous phase and liberate small molecular segments, which diffuse towards the crystals surface and initiate chemicrystallisation.[10] The Fayolle model predicts the degree of crystallinity as a function of aging time. Required input includes the initial crystallinity χ_{c0}, molecular weight evolution $M_n(t)$, and entanglement molecular weight M_e:[10]

$$\chi(t)=\chi_{c0}+\frac{1-\chi_{c0}}{\left[\left(\frac{M_{n0}}{M_e}\right)^{\frac{1}{2}}-1\right]}\left[\left(\frac{M_{n0}}{M_n(t)}\right)^{\frac{1}{2}}-1\right] \quad (2)$$

Stage 2 to Stage 3: Scale Bridging. Individual models are designed to function in a specific scale range. In order to couple single-scale models and develop larger multiscale model a scale bridging procedure is required. In the case of the degradation model proposed here only one such procedure is needed. The dependence of the glass transition temperature on molecular weight $T_g(M_n)$ must be found to integrate the kinetic model with the structure–property relationship. $T_g(M_n)$ can be obtained with the Fox and Flory equation:[9,11]

$$T_g(M_n)\approx T_g^{\infty}-0.002715\ \frac{\left(T_g^{\infty}\right)^3}{M_n} \quad (3)$$

where T_g^{∞} is the hypothetical T_g for infinite molecular mass. T_g^{∞} is a material parameter that can be calculated substituting the initial T_g and M_n into the former equation.

Stage 3: Structure–Property Relationship. The microstructure–property relationship yielding local mechanical properties of the polymer must be found. The multiscale approach proposed here used topological formalism utilizing connectivity indices defined via graph theoretical concepts as primary descriptors of the polymer repeat units. Topology can be seen as a pattern of interconnections between atoms in a polymer repeat unit. Connectivity indices give information on the electronic configuration and the coordination number for all atoms in the monomer.[9]

In order to quantitatively predict polymer properties from the microstructural data connectivity parameters are correlated with the experimental results of so called fundamental properties.[9] Fundamental material properties are properties in the microscale such as volume occupied by the molecule, cohesive energy, etc. They are further combined into derived properties on the macroscale such as density or elastic constants.[9] Formulas for derived properties are obtained by fitting the experimental data with equations from thermodynamic and molecular theories.

It is argued that this method is more practically feasible than alternative approaches, e.g., molecular dynamics simulations or group contribution technique. Molecular dynamics must deal with time limitation and scale bridging issues.[12–14] Group contribution technique cannot be used if estimating the value of even a single group contribution is problematic. This serious limitation actually triggered the development of the topological approach.[9,15]

The structure of the PA11 repeat unit was analyzed to obtain the topology data.[9] The following values of the connectivity indices were found and will be used in the model:[9]

$$X_0=9.3555,\quad X_0^V=8.4793$$
$$X_1=6.3938,\quad X_1^V=5.6612 \quad (4)–(7)$$

Generally X_0 and X_1 provide information on coordination numbers while X_0^V and X_1^V quantify details of the electronic configuration in the monomer.

The exact procedures required to get the structure–property relationships in the Stage 3 are different for each property to be obtained. They are described in detail for the mechanical properties in the later parts of this article. The model for morphology predictions was already featured in the previous article.[5]

Stage 4: Global Properties. In the final stage the local properties must be combined into global engineering parameters. This can be done with several methods such as micromechanical finite element analysis or composites theory, e.g. Halpin and Kardos.[16]

Table I. Constituent Models of Multiscale Approach for Prediction of Various Properties

Property modeled (multiscale approach)	Constituent models
Modulus	Jacques[2]
	Fox and Flory[2,3]
	Bicerano[2,3] topological
	Seitz[3]
	Rubber[3] elasticity
	Crystallinity multiscale[3]
	Halpin-Tsai[3]
	Water softening[3]
Tensile strength	Jacques[2]
	Fox and Flory[2,3]
	Bicerano[2,3] topological
	Wu[3]
	Seitz[3]
	Halpin-Tsai[3]
Embrittlement	Jacques[2]
	Fox and Flory[2,3]
	Bicerano[2,3] topological
	Seitz[3]
	Tensile strength multiscale[2,3]
	Kausch[2-4]
Mechanical equilibrium[a]	Modulus[3] amorphous multiscale
	Crystallinity[3] multiscale
	Halpin-Tsai[2,3]

[a] Molecular weight as an independent variable; numbers indicate stage or scale bridging in which certain model was introduced—reference in the main text.

In the case of PA11 aging described here there is an even distribution of water through the body as the diffusion happens very quickly. Besides this the current modeling approach has seen the amorphous matrix as perfectly homogenous with evenly distributed crystallites. Therefore properties will be uniform throughout the material and global engineering properties do not need to be evaluated. Because of this Stage 4 will not be considered at any point later in the article.

PREDICTION OF THE PA11 MECHANICAL PROPERTIES

This section contains detailed property prediction procedures for the Young's modulus, yield strength, embrittlement, and mechanical equilibrium. It also features comparison between model and experiment. An analogous section in Part 2 of this article series considered the density and crystallinity evolution.[5]

Experimental results relevant for the modeling described here were reported in detail in previous work.[6] They are reported with error bars representing one standard deviation of parallel laboratory test results. It is supposed to give a statistically meaningful comparison between model predictions and laboratory testing.

Input and Output Parameters

Table I lists the constituents of multiscale models applied in this article to calculate mechanical properties of PA11. Table II features input parameters for these constituent models, their values to be used with the property predictions along with reference and the output parameters produced by the model.

Input parameters can be generally divided into constants and variables. The constants are the parameters specific for a certain polymer system. The variables describe conditions specified by the application. Such variables include aging conditions (hydrolysis temperature and time), initial parameters of the studied sample (initial molecular weight and degree of crystallinity), and finally test temperature in the case of tensile mechanical properties.

Predicting Elastic Modulus

The decrease in amorphous Young's modulus due to chemical action can be estimated by taking into account the rate of chain scission from stage two of the present methodology and by relating it to the number average molecular weight. Then the change in the glass transition temperature can be found and used to express Poisson's ratio and finally elastic constants of the polymer.[20,21]

The procedures to calculate the polymeŕs elastic modulus of the amorphous phase in three different temperature regimes (glassy, rubbery, and leathery state) have been established.[9] Subsequently the obtained amorphous modulus, the assumed crystalline modulus and the previously calculated crystallinity evolution $\chi(t)$ have been combined with the Halpin-Tsai short fiber composite model.[16] The crystalline phase is considered impenetrable to water,[1] therefore it is expected to have constant morphology and properties during degradation. Moreover the present study followed the approximation used in El-Mazry's work.[10] It was assumed that the secondary lamellae created in the process of chemicrystallization possess the physical and thermal characteristics of the initial primary lamellae.

The modulus calculation procedure is described below showing the steps that must be taken and stages they belong to:

Input from Microscale Models.

- Step 1. First the specific volume must be obtained as described in "Predicting Density" chapter of the previous article[5] (Part 2). Conditions corresponding to different polymer states are as follows:
  - Glassy state for:
$$T \leq Tg,\ Tg > 298\,\mathrm{K}$$
  - Rubbery state for:
$$T > Tg,\ Tg > 298\,\mathrm{K}$$
or
$$T > Tg,\ Tg \leq 298\,\mathrm{K}$$
- Step 2. Entanglement molecular weight M_e and $\chi(t)$ are calculated as described in "Predicting Crystallinity" section of the previous article[5] (Part 2).

Table II. Input Parameters, Their Values, and Output of Constituent Models in Multiscale Approach

Model	Input parameters	Values chosen	Output parameters
Jacques	T_{hyd}—hydrolysis temperature	120°C—slightly above riser working conditions[2]	$M_n(t)$—number average molecular weight
	M_{n0}—initial molecular weight	40.64 kg/mol—experiment[6] (part 1)	
	t—hydrolysis time	Independent variable	
Fox and Flory	T_g^{MW}—initial T_g for specified molecular weight	45°C for 40.64 kg/mol—literature[2] T_g for M_{n0}	$T_g(M_n)$—glass transition temperature
	$M_n(t)$	Jacques model	
Bicerano topological	$T_g(M_n)$	Fox and Flory model	E_{coh}, V_w, V, M_e, φ_a—see input parameters below
	Connectivity	X_0=9.3555 X_0^V=8.4793, X_1=6.3938, X_1^V=5.6612 from literature[9]	
	M—monomer mass	174.2 g/mol from literature[9]	
	l_m—monomer length	14.05 Å—self-calculated from geometry of monomer	
	T—test temperature	25°C—Room temperature assumed	
	$T_g(M_n)$	Fox and Flory model	$B(T)$, $E(T)$, $G(T)$—bulk, Young's and shear moduli for glassy state $\sigma_f(T)$—brittle fracture stress
	E_{coh}—cohesion energy	84.7 kJ/mol—Bicerano model	
Seitz	V_w—Van der Waals volume	119.8 cm^3/mol—Bicerano model	
	V—specific volume at test temperature	185.4 cm^3/mol—Bicerano model	
Rubber elasticity	M_e—entanglement molecular weight + Same as Seitz model	2.27 kg/mol—Bicerano model	$B(T)$, $E(T)$, $G(T)$—bulk, Young's and shear moduli for rubbery state
Fayolle	X_{c0}—initial crystallinity ratio	21.7%—experiment[6] (part 1)	$X_c(t)$—degree of crystallinity
	M_{n0}, $M_n(t)$	Jacques model	
	M_e	Bicerano model	
Halpin-Tsai	E_a—amorphous phase modulus	Seitz model	E_{sc}—modulus of the semicrystalline polymer
	E_c—crystalline phase modulus	25 GPa[a]—literature[17]	
	$X_c(t)$	Fayolle model	
	A_f—crystalline phase aspect ratio	1—ideal spherulites assumption	
Wu	$T_g(M_n)$	Fox and Flory model	σ_a—amorphous tensile strength
	E_{coh}, V	Bicerano model	
	C_∞—characteristic ratio	5.95[b]—literature[18]	

Table II. *Continued*

Model	Input parameters	Values chosen	Output parameters
Water softening	E_{sc}	Halpin-Tsai model	E_{sat}—modulus corrected for water or plasticizer content
	k_{sat}—water softening factor (saturated state)	0.78—obtained from E (wt %) relation[c], literature[19]	
	k_{bnd}—softening factor of "bound water"[d]	0.93—obtained from E (wt %) relation[c], literature[19]	
	k_{res}—softening factor of the residual plasticizer[e]	0.82—obtained from reported $E_{plast} - E_{unplast}$[f], literature[2]	
Kausch	M_e	Bicerano model	$MW_e^{brittle}$—embrittlement threshold

[a] α form of PA6—expected similar to PA11.
[b] For PA66.
[c] Softening effect of certain water content is assumed the same for all polyamides (difference arises solely from variation in saturation rates and levels).
[d] As in Langmuir desorption model[19] (0.5% assumed).
[e] 2% assumed, experiment[6] (part 1).
[f] Softening effect of plasticizer is assumed linear with respect to its content,literature.[19]

Stage 3: E(t) Amorphous. ***Glassy state.*** The bulk modulus and Poisson's ratio formulas for a glassy state polymer operate in the temperature range of:[9]

$$T \leq Tg - 20\,\mathrm{K}, \quad Tg > 298\,\mathrm{K}$$

For the minor case of $T \leq Tg - 20\,\mathrm{K}$, $Tg \leq 298\,\mathrm{K}$ there are no correlations with proven accuracy.[9]

- Step 3. The bulk modulus is calculated as a function of specific volume and topology of a monomer:[9]

$$B(T) \approx 8.23333 \; E_{\mathrm{coh1}} \left[\frac{5V(0K)^4}{V(T)^5} - \frac{3V(0K)^2}{V(T)^3} \right] \tag{8}$$

where E_{coh1} is the Fedor's type cohesive energy (J/mol).

The cohesive energy can be expressed with the following formula:

$$E_{\mathrm{coh1}} = 9882.5 \; X_1 + 358.7 \; \left(6\,N_{\mathrm{atomic}} + 5\,N_{\mathrm{group}}\right) \tag{9}$$

N_{atomic} and N_{group} are the correction terms that can be calculated as follows:

$$N_{\mathrm{atomic}} = 4N_{(-S-)} + 12N_{\mathrm{sulfone}} - N_{\mathrm{F}} + 3N_{\mathrm{Cl}} + 5N_{\mathrm{Br}} + 7N_{\mathrm{cyanide}} \tag{10}$$

where: $N_{(-S-)}$—number of sulfur atoms in the lowest oxidation state, N_{sulfone}—number of sulfur atoms in the highest oxidation state, N_{F} , N_{Cl}, and N_{Br}—total numbers of fluorine, chlorine, and bromine atoms, N_{cyanide}—number of nitrogen atoms with $\delta = 1$ and $\delta^V = 5$.

$$\begin{aligned} N_{\mathrm{group}} &= 12N_{\mathrm{hydroxyl}} + 12N_{\mathrm{amide}} \\ &+ 2N_{[\mathrm{non-amide\text{-}(NH)-unit}]} - N_{(\mathrm{alkyl\ ether-O-})} - N_{\mathrm{C=C}} \\ &+ 4N_{[\mathrm{non-amide\ -(C=O)-\ next\ to\ nitrogen}]} \\ &+ 7N_{\left[\begin{array}{c}\mathrm{-(C=O)-in\ carboxylic\ acid,\ ketone\ or} \\ \mathrm{aldehyde}\end{array}\right]} + 2N_{[\mathrm{other-(C=O)-}]} \\ &+ 4N_{\left(\begin{array}{c}\mathrm{nitrogen\ atoms\ in\ six\ membered} \\ \mathrm{aromatic\ rings}\end{array}\right)} \end{aligned} \tag{11}$$

where N_{hydroxyl} denotes the total number of −OH groups in alcohol or phenol environments and N_{amide} is a total number of amide groups.

For PA11 $N_{\mathrm{group}} = 12$ and $E_{\mathrm{coh1}} = 84.7 \frac{\mathrm{kJ}}{\mathrm{mol}}$. Several atom types have been found to correlate in the general case with E_{coh1}, but it is irrelevant for PA11 since $N_{\mathrm{atomic}} = 0$.

The expression for the bulk modulus was obtained from molecular and thermodynamic considerations.[20] Polymer repeat units were assumed to be surrounded by a mean field as described by the Lennard-Jones potential function:[22]

$$V(r) = 4\varepsilon \left[\left(\frac{\sigma}{r}\right)^{12} - \left(\frac{\sigma}{r}\right)^{6} \right] \tag{12}$$

where $V(r)$ is the intermolecular potential between the two molecules, ε is the potential well depth, σ is the van der Waals

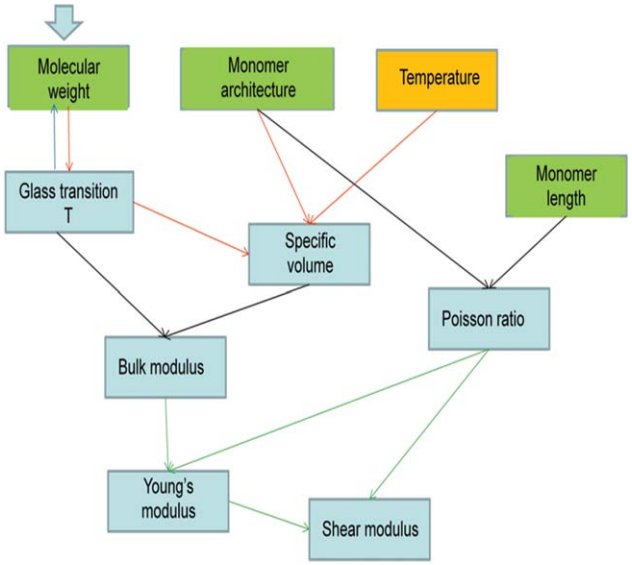

Figure 1. Flow chart for the modulus calculation. Green boxes are related to the architecture of the molecule and blue boxes describe the macro properties of the polymer. [Color figure can be viewed in the online issue, which is available at wileyonlinelibrary.com.]

radius, and r is the distance of separation between both particles.

Based on this the total potential energy of a system was defined and its partial derivative with respect to the specific volume was obtained. The latter was then substituted into the thermodynamic equation state for pressure P below the glass transition temperature. Finally by taking the derivative of the pressure and multiplying the result by the specific volume (since $B=-V[(\mathrm{d}P)/(\mathrm{d}V)]_T$)[20] an expression for the bulk modulus as a function of fundamental properties is obtained.

- Step 4. The Poisson's ratio $v(T)$ is calculated as a function of T_g, temperature, connectivity indices and monomer length:[9]

$$v(T) \approx v_0 + \frac{50T}{T_g}\left\{0.00163+\exp\left[0.459\left(T-T_g-13\right)\right]\right\} \quad (13)$$

$$v_0 = v(298\,\mathrm{K}) - \frac{14,900}{T_g}\left\{0.00163+\exp\left[0.459\left(285-T_g\right)\right]\right\} \quad (14)$$

$$v(298\,\mathrm{K}) = 0.513 - 3.054\times10^{-6}\sqrt{\frac{V_w}{l_m}} \quad (15)$$

where V_w is the van der Waals volume (mL/mol) and l_m is a monomer length in its fully extended conformation (cm).

$v(T)$ was obtained as a fitting function between the experimental Poisson's ratio and temperature, v_0 is merely used to simplify the notation.[20] $v(298\,K)$ was obtained as a fit between the experimental Poisson's ratio at room temperature and the cross-sectional area of the polymer repeat unit.[20]

- Step 5. Young's and shear moduli are expressed in relation to the bulk modulus and Poisson's ratio

Finally the Young's modulus is found from elasticity theory for isotropic materials:

$$E = 2(1+v)G = 3(1-2v)B \quad (16)$$

Properties here are assumed isotropic at the local level.

Figure 1 summarizes the calculation of the elastic moduli in a form of a flow chart. It shows that from the architecture of the macromolecule (green), the temperature (orange) and the initial T_g it is possible to calculate a wide range of polymer properties (blue).

Rubbery state. The rubbery state formulas mentioned in this paragraph function in the temperature range $T \geq Tg+30\,\mathrm{K}$ for the shear and bulk modulus and $T \geq Tg$ for Poisson's ratio. They are obtained from rubber elasticity theory as discussed in Ref. 9.

- Step 3. The shear modulus is calculated as a function of temperature, density, specific volume, and M_e:

$$G_N^0(T) = \frac{\rho(T)\times RT}{M_e}(\mathrm{Mpa}) \quad (17)$$

$$\rho(T) = \frac{M}{V(T)}(\mathrm{g/mL}) \quad (18)$$

The modulus is here defined only for temperatures in the rubbery plateau regime, inception of which is assumed to be at $(Tg+30\,\mathrm{K})$. This expression does not apply to temperatures in the terminal zone, where a steep decrease of modulus occurs.[9] Since the onset of the terminal zone is not clearly defined, a practical approach often involves calculating the modulus for the inception point $(Tg+30\,\mathrm{K})$ and assuming the obtained value for an arbitrary rubbery plateau.[9]

- Step 4. The bulk modulus is calculated from the specific volume and connectivity indices

$$B(T) = \frac{\frac{205V(T)}{V_w}}{\left[\frac{V(T)}{V_w}-1.27\right]^2} - 2329\left[\frac{V_w}{V(T)}\right]^2 \quad (19)$$

where V_w is the van der Waals volume.

The expression for the bulk modulus in the rubbery state was obtained in an analogous way to the glassy state. The thermodynamic equation of state for pressure P above the glass transition temperature was used.

- Step 5. The Poissońs ratio is obtained from the bulk and shear moduli

$$v = \frac{3B(T)-2G(T)}{6B(T)+2G(T)} \quad (20)$$

- Step 6. The Young's modulus is obtained from the shear modulus and Poisson's ratio

$$E(T) = 2[1+v(T)]\times G_N^0(T) \quad (21)$$

Leathery state. Between the glassy and rubbery domain the transition "leathery" period can be identified. This is modeled as a linear interpolation between the left boundary considered glassy and a right one assumed rubbery:

$$\text{For:}\quad T_g - 20\ \text{K} < T < T_g + 30\ \text{K}$$

$$E(T) = E_{Tg-20\text{K}} - \frac{E_{Tg-20\text{K}} - E_{Tg+30\text{K}}}{50\text{K}}\left(T - T_g + 20\,\text{K}\right) \tag{22}$$

Stage 3: E(t) Semicrystalline. ***Halpin-Tsai model.***

- Step 1. The Young's modulus of the amorphous phase is taken from the topological approach for either the glassy, the rubbery, or the leathery state. The crystalline modulus is taken from the literature.[17] It is assumed not to change due to the exposure to water, because water does not penetrate the crystalline region.

$$E_a(t) \leftarrow \text{Elastic modulus model (glassy, rubbery, or leathery)}$$
$$E_c = 25\ \text{GPa},\ \text{constant} \tag{23}$$

- Step 2. The Halpin-Tsai short fiber composite model combines moduli of the two phases and the crystallinity change $\chi(t)$ into a global modulus of the material:[16]

$$E_l(t) = E_a(t)\ \frac{1 + (2A_f)\eta_l\chi(t)}{1 - \eta_l\chi(t)} \tag{24}$$

$$\eta_l = \frac{(E_c/E_a) - 1}{(E_c/E_a) + 2A_f} \tag{25}$$

$$A_f = l_f / d_f \tag{26}$$

where E_l—longitudinal modulus of the material, A_f—aspect ratio of the crystallite, l_f—average length of the crystallite, d_f—average diameter of the crystallite.

Because crystallites are assumed to be perfect spherullites $A_f = 1$ in this approach: $E_l = E_t = E_{\text{random}}$.

Softening effect of water saturation. Water is known to act in a similar way as a plasticizer, thus its absorption shall have a softening effect.[19] An empirical relationship with regard to the softening can be written in the form of:

$$E_{\text{sat}}(t) = k(t) \times E_0 \tag{27}$$

where $E_{\text{sat}}(t)$—Young's modulus of water saturated semicrystalline polymer, E_0—initial Young's modulus of semicrystalline polymer, $k(t)$—time dependent softening factor obtained from experimental study of isothermal water absorption.[19]

The above can be also used for other plasticizers as long as experiments necessary to obtain $k(t)$ have been performed. A summary of relevant softening factors is given in Table II.

The multiscale model used here estimates the effect of plasticizer for PA11. It incorporates experimental results reporting as much as 2% of remaining plasticizer after exposure in 120°C and a relative difference in the modulus between plasticized and unplasticized PA11 as given in the Rilsan documentation.[2,6] The assumption of the linear softening with respect to plasticizer content is based on water induced softening, which was found to be nearly linear before reaching a modulus plateau region.[19]

Elastic Modulus Evolution

The Young's modulus obtained from the modeling has been compared with an experimental stress strain curve measured at a displacement rate of 2 mm/min. The secant modulus was calculated as the slope between 0.2% and 0.5% strain according to common practice in polymer science. The modulus was also obtained as the storage modulus tested at 2 Hz in a Dynamic Mechanical Thermal Analysis (DMTA). Samples used were aged more than 7 days to assure effects of plasticizer become largely reduced and they were subsequently dried. Figure 2 summarizes the comparison between the multiscale model and experiment (tensile test, DMTA) for the Young's modulus.

The predicted modulus is in good agreement with the experimental results from the DMTA test, but it is significantly overestimated compared with the tensile test. Since the tensile test is done at a much lower strain rate than the DMTA testing a change in modulus is to be expected for a viscoelastic polymer.

The multiscale model calculates the theoretical Young's modulus; however, it does not distinguish between different deformation modes and it does not account for loading rate dependent properties. Within the model presented here tensile, flexural and storage moduli should all yield the same value. The parameters used in this model were typically obtained for testing rates of the DMTA. The T_g reported here for PA11 is a key parameter obtained by DMTA. T_g is loading rate dependent and this aspect has not been modeled. It is, therefore, reasonable that the dynamic storage modulus better accounts for the viscoelastic nature of polymers than the modulus obtained from the standard tensile test.

The experimental data (taken with uncertainty values) can be interpreted as monotonically increasing with an eventual plateau and this characteristic is well predicted with the model. Therefore, chemicrystalization and chain scission are confirmed as the two governing mechanisms of stiffness evolution (following additive extraction). Some discrepancy between the model and DMTA result occurs only for the first week of aging, since at this time a significant amount of plasticizer is still in the sample. A possible sharp stiffness increase between 4 and 6 weeks of aging (as observed for the tensile modulus) has been ruled out after subsequent DMTA tests.

If only the tensile data is available the model can be directly used to estimate the time to reach the modulus plateau during hydrolysis. As a practical approach it could also be possible to measure the tensile modulus experimentally, which can be easily done. The change of the modulus with time can then be predicted with the theory described here. Including viscoelastic effects and using time temperature superposition is planned for the future.

Predicting Tensile Yield Strength

The multiscale model predicting yield strength incorporates the Wu equation for the amorphous phase coupled with a computational procedure (converting tensile strength into modulus via an empirical relation, calculating global modulus with Halpin-Tsai equations and finally converting it back to strength) for a

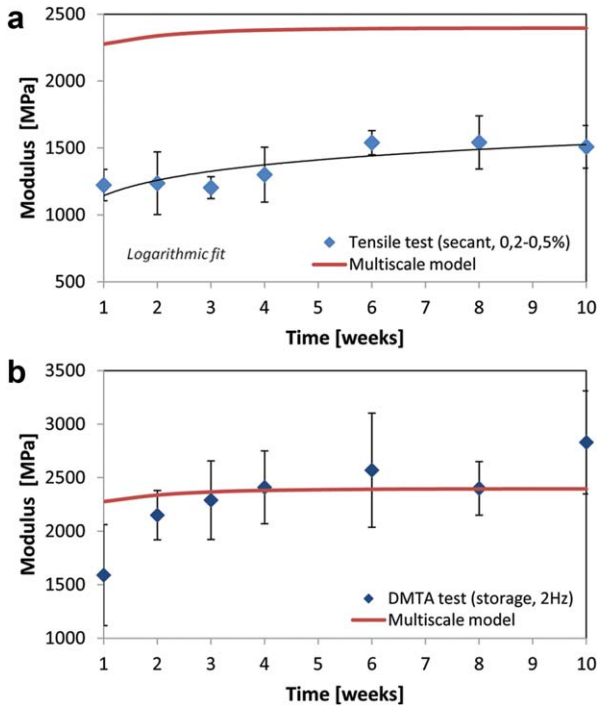

Figure 2. Comparison between modeled and experimental Young's modulus of the water saturated samples in (a) static tensile and (b) dynamic mechanical deformation. [Color figure can be viewed in the online issue, which is available at wileyonlinelibrary.com.]

semicrystalline polymer. The effect of water and residual plasticizer was neglected.

This method considers glassy polymers at temperatures of at least 20°C below their glass transition temperatures.

The tensile yield strength calculation procedure is described below:

- Step 1. T_g, E_{coh1}, and $V(T)$ are calculated as described in the previous sections. The characteristic ratio of polymer macromolecule C_∞ and crystalline modulus E_c are obtained from the literature.[17,18]

Stage 3: $\sigma_a(t)$.

- Step 2. The amorphous tensile yield strength is calculated from the Wu model:[9]

$$\sigma_a(t) = 10^{(-3.36+C_\infty)}\left(T_g - T\right)\left(\frac{E_{\mathrm{coh1}}}{V(T)}\right) \tag{28}$$

The yield stress σ_a has been shown to be proportional to $\Delta T = T_g - T$ and $\frac{E_{\mathrm{coh1}}}{V(T)}$, where T is the testing temperature and $\frac{E_{\mathrm{coh1}}}{V(T)}$ the cohesive energy density.[23] This proportionality is due to interchain effects on the yield stress. At the yield point of tensile deformation some bonds start to rotate from *cis* to *trans* conformation causing irreversible extension of some chains segments. Therefore experimental values of the yield stress were plotted against intrinsic chain flexibility quantified by the characteristic ratio C_∞ in order to obtain the final formula.[23]

Stage 3: $\sigma_{sc}(t)$.

- Step 3. The tensile yield stress of the amorphous phase is converted to Young's modulus via an empirical relationship,[9] the crystalline modulus is again taken from the literature[17]

$$E'_a = \frac{\sigma_a(t)}{0.028} \tag{29}$$

$$E_c = 25 \text{ GPa, constant}$$

- Step 4. The Halpin-Tsai short fiber composite model is combining moduli of the two phases into a global modulus of the material:[16]

$$E_l(t) = E'_a \frac{1+(2A_f)\eta_l\chi(t)}{1-\eta_l\chi(t)} \tag{30}$$

where E'_a is a amorphous tensile strength converted to modulus.

- Step 5. The modulus is converted back to strength obtaining an estimate for the semicrystalline polymer:

$$\sigma_{sc}(t) = E_l(t) \times 0.028 \tag{31}$$

Tensile Strength Evolution

The experimental tensile strength was obtained by dividing the maximum load in each stress–strain curve by the original cross-sectional areas. Figure 3 summarizes the tensile strength comparison between the multiscale model and tensile test results. Predicting tensile strength turns out to be less problematic than it is the case for the tensile elastic modulus. Here the exact strength values as well as their change with time are modeled fairly well.

The multiscale model incorporating the crystalline phase predicts the experiments much more closely in both absolute value and trend than one for the amorphous phase only. This suggests that the crystalline phase does play an important role in the plastic deformation as opposed to the view that this is solely a matter of the amorphous phase. The above hypothesis could be experimentally tested in the future by qualitatively comparing the shape of crystallites in undeformed and deformed samples.

Predicting Embrittlement

Polymeric materials often undergo embrittlement during chemical degradation. Two semiempirical methods estimating the M_n at which the aged material becomes brittle are proposed here. The models give rough estimates of embrittlement conditions.

Yielding and Brittle Fracture Balance. The yielding-brittle fracture balance method uses local properties of the material (stage 3) to obtain the molecular parameter (stage 2) tied with macroscopic behavior of embrittlement. The embrittlement threshold calculation procedure employing this method is described below:

- Step 1. The specific volume is calculated as described in previous sections.
- Step 2. Brittle fracture of the semicrystalline polymer is calculated as a function of specific volume and monomer length:[9]

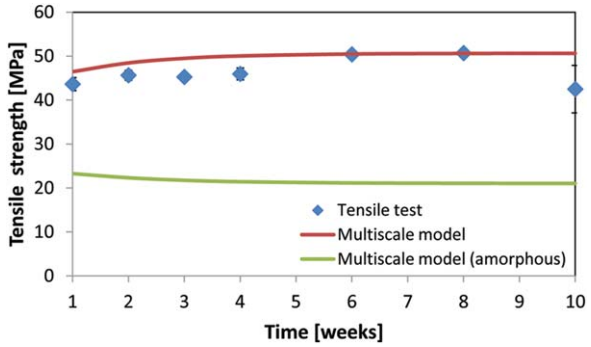

Figure 3. Comparison between modeled and experimental tensile strength evolution. [Color figure can be viewed in the online issue, which is available at wileyonlinelibrary.com.]

$$\sigma_f(T) \approx \frac{2.288424\times10^{11}\times l_m}{V(T)} \tag{32}$$

The brittle stress to failure is given by the number of bonds times the strength of an individual bond minus the effect of structural defects concentrating high stress in local areas.[20] Therefore, plotting the number of backbone bonds per unit area against the measured brittle strength and a subsequent regression analysis yield the theoretical strength of a fully extended (M_w^{∞}) linear polymer. Subsequently, the $\frac{Mw}{Me}$ ratio at which the strength goes to zero was used to obtain the molecular weight dependent brittle fracture stress from the theoretical stress.[20]

- Step 3. The yield stress of the semicrystalline polymer is calculated with the procedure involving the Wu equation:

$$\sigma_y(T) \leftarrow \text{tensile strength model}$$

- Step 4. A lower value stress is assigned as a governing mechanism

$$\sigma_f(T) > \sigma_y(T) \text{ or } \sigma_f(T) < \sigma_y(T)$$

- Step 5. The embrittlement threshold is estimated.

Embrittlement happens, when the time of exposure causes a reduction of molecular weight $\left(\mathrm{MW}_{y-f}^{\mathrm{brittle}}\right)$ for which the criterion $\sigma_f(T) < \sigma_y(T)$ is reached.

This method takes crystallinity into account by using yield strength values (dependent on crystallinity ratio).

Cohesion Based Evaluation. Macromolecules inside the polymer can move apart easily, when cohesion is low. This means they eventually get completely separated. When the same force is exerted to material with high cohesion, the molecules would still stick together. In polymers the entanglement network creates an important part of intermolecular cohesion forces, determining the plastic deformation responsible for ultimate elongation.[10] When the number of entanglements per macromolecule decreases due to degradation, the Van der Waals interactions remain as the main intermolecular forces. The Van der Waals forces alone are not strong enough for allowing plastic deformation. This stage marks the onset of a brittle material.

An appropriate criterion has been developed by Kausch:[24]

$$\mathrm{MW}_e^{\mathrm{brittle}} \approx 5\,M_e \tag{33}$$

The entanglement molecular weight has been estimated with the topological model. This method converts the microstructural parameter (stage 2) to a molecular parameter tied to macroscopic behavior of embrittlement.

In the cohesion based evaluation crystallinity is neglected as influencing brittle fracture. The embrittlement is considered to happen because of weak intermolecular forces in the amorphous phase. Consequently, once the amorphous phase gets brittle there is nothing to hold the crystalline parts together anymore.

Embrittlement Threshold Evaluation

The first of the embrittlement predicting methods proposed here calculates the molecular weight for which yielding and fracture stresses are equal marking the onset of PA11's brittle failure domain:

$$\mathrm{MW}_{y-f}^{\mathrm{brittle}} \approx 9.2\,\mathrm{kg/mol} \tag{34}$$

The second method calculates molecular weight for which PA11 entanglement network is no longer able to allow plastic deformation:

$$MW_e^{brittle} \approx 11.4\,\mathrm{kg/mol} \tag{35}$$

These modeled values can be compared with the experimentally established Corrected Inherent Viscosity (CIV) based failure criterion of 1.05 dL/g as given in the American Petroleum Institute (API) standard.[1] The viscosity value can be converted to molecular weight with Jacques equation:[8]

$$\mathrm{MW}_{\mathrm{API}}^{\mathrm{brittle}} \approx 13.8\mathrm{kg/mol} \tag{36}$$

$\mathrm{MW}_{\mathrm{API}}^{\mathrm{brittle}}$ is an industrial, experience based criterion giving a molecular weight below which PA11 exhibits brittle behavior. The modeled embrittlement thresholds mark the minimum molecular weight for which any plastic deformation is theoretically possible. The plateau for PA11 hydrolysis is about 17 kg/mol[6]—corresponding to initial service acceptance criterion of 1.2 dL/g given by API.[1,8] This means that brittle fracture usually involves additional mechanisms of chain scission.

The two models described above are semiempirical and more work is needed to determine which approach is best. Also, the experimental embrittlement definition used in the API standard is not ideal. However, the advantage of the theoretical methods given above is their ability to estimate a rough preliminary brittle failure criterion of various polymers without the need for extensive testing as in the conventional CIV-mechanical method described by API.

Predicting Mechanical Equilibrium

Following plasticizer depletion the stiffness evolution is modeled as a competition between degradation of the amorphous phase and an increasing crystallinity ratio. Initially mechanical properties are controlled by chemicrystalization, however, the chain scission gradually takes control over time.

Mechanical equilibrium is here defined as the molecular weight $\mathrm{MW}_{\mathrm{mech}}^{\mathrm{eq}}$ corresponding to a point on a stiffness versus time curve,

where effects of degradation and chemicrystalization on the modulus cancel each other out. This is also the molecular weight for which the maximum modulus point during aging occurs. After crossing that point of time degradation takes control. Mechanical equilibrium has been found by observing how the modeled elastic modulus changes with decreasing molecular weight directly rather than indirectly via time and the kinetic model.

Mechanical Equilibrium Evaluation

Equilibrium of degradation and chemicrystalization effects on PA11 stiffness is predicted here as:

$$\mathrm{MW}_{\mathrm{mech}}^{\mathrm{eq}} \approx 10.8 \text{ kg/mol} \quad (37)$$

This is molecular mass for which the highest value of modulus is obtained during aging. A further decrease of molecular weight would see chain scission taking control over stiffness changes. This does not happen for the studied samples, since the hydrolysis plateau is around 17 kg/mol.[6] However, it may happen if additional degradation mechanisms are involved, such as oxidation or UV exposure.

DISCUSSION

In general the model presented here is best understood as a practical tool providing engineers with fast and accurate predictions of mechanical properties. The model is not only accurate, but also particularly easy to use due to the analytic form of its formulas. The fundamental input parameters are available for most common polymers in the literature. The proposed approach can be applied to every polymer as long as a kinetic model for the specific chemical process in the specific material is known. Such models exist for a wide range of practically important degradation processes in various materials.

Input parameters for the mechanical properties predictions can be obtained relatively easy. Information needed for the structure–property relationship of the amorphous phase (connectivity, mass and length of the polymer repeat unit) can be directly obtained from the architecture of the polymer's repeat unit. Parameters such as initial molecular weight M_{n0} and initial degree of crystallinity χ_{c0} depend on the studied specimen. M_{n0} can be evaluated with viscometric[1] and spectrometric[25] measurements while by χ_{c0} may be obtained with XRD,[26] DSC,[6,10] FT-IR,[10] and density[6,26] tests. The glass transition temperature T_g is a material constant available in the literature for numerous polymers.[2,9] The model could probably be improved by considering the rate dependence of T_g. The quantities such as the modulus of the crystalline phase E_c and the characteristic ratio of macromolecules C_∞ are more difficult to find for every polymer. In this case, as a practical approach, values for the closest known material should be assumed. Here the crystalline modulus of commonly used PA6 was taken as a proxy for PA11. Moreover the model ignores any possible effects of parameters like crystallite size, distribution, and orientation or molecular weight distribution. It should be possible to develop the model further and consider these effects in detail. Predictions should also improve once better input data is available. Nevertheless, the good match between the model and experiment indicates that the approach taken here is sufficiently accurate for Polyamide 11.

The main limitation of the proposed model is its semiempirical nature. Consequently the model cannot provide any theoretical understanding of property emergence from the structure in the microscale. It did, however, bring some insights into the workings in larger scales, e.g. it evaluated the role of crystallites in the plastic deformation and proposed the existence of a mechanical equilibrium. The theory does not account for the modulus strain rate dependence, which corresponds to testing at the arbitrary "standard" rate. Predictions may therefore deviate from experiment in extreme cases, however high accuracy has been obtained in literature for commonly used loading rates.[9] Moreover the model does not have any theoretical basis to evaluate the effects of plasticizers and it is best applicable to dried specimens. Nevertheless for important polymers, water absorption[19] (acting as plasticizer) and plasticizer extraction[2] have been linked to changes of the mechanical properties. Therefore, empirical softening factors can be used to estimate the properties of water saturated samples with residual plasticizer content in place. Results for Polyamide 11 suggest that this produces predictions relevant from practical point of view.

CONCLUSIONS

Multiscale modeling results have been compared with experiments for PA11 hydrolysis during water exposure in 120°C. Experiments were shown in the initial article of the series (Part 1). The model was divided into an article describing morphological parameters during degradation (Part 2), as reported previously, and this work treating the mechanical properties (Part 3).

For all tested properties the modeled trend is close to the experimental results. This similarity confirms that the modeling approach chosen here gives relevant results. It also confirms that hydrolysis induced chain scission and chemicrystalization are the two main mechanisms of property change, because these two mechanisms are central to all modeling used. A very good match between model and experiment has been already reported in the case of density and crystallinity evolution. In this work equally good predictions were found for the tensile yield strength, storage modulus and embrittlement threshold.

Results for the tensile strength suggest that the crystalline phase does play a role in plastic deformation as opposed to the view that this is solely a matter of the amorphous phase. The model predicted the existence of mechanical equilibrium between effects of macromolecule degradation and increased degree of crystallinity.

The results suggest that the multiscale modeling methodology can provide faster and less labor extensive alternatives for accelerated aging tests when it comes to long-term property evaluation.

ACKNOWLEDGMENTS

This work is a part of the "PolyLife" project realized between SINTEF Materials and Chemistry, NTNU, PETROBRAS, ROSEN Group, Kongsberg Oil & Gas Technologies, and FMC Technologies. The authors express their gratitude for the financial support by the Research Council of Norway (grant 193167). Randi Berggren performed accelerated aging and mechanical tests as part of her master thesis at NTNU.

REFERENCES

1. API Technical Report 17TR2. The Ageing of PA-11 in Flexible Pipes; API Publishing Services: Washington, DC, **2003**.
2. Rilsan® PA11: Created From a Renewable Source; Arkema: France, **2012**.
3. Teal, J. M.; Howarth, R. W. *Environ. Manage.* **1984**, *8*, 27.
4. Flynn, J. H. *J. Therm. Anal. Calorimetry* **1995**, *44*, 499.
5. Mazan, T.; Jørgensen, J. K.; Echtermeyer, A. T. *J. Appl. Polym. Sci.* **2015**, *132*, 12039.
6. Mazan, T.; Berggren, R.; Jørgensen, J. K.; Echtermeyer, A. T. *J. Appl. Polym. Sci.* **2015**, *132*, 6249.
7. Wu, P.; Siesler, H. W. *Chem. Mater.* **2003**, *15*, 2752.
8. Jacques, B.; Werth, M.; Merdas, I.; Thominette, F.; Verdu, J. *Polymer* **2002**, *43*, 6439.
9. Bicerano, J. Prediction of Polymer Properties; Marcel Dekker AG: New York, **2002**.
10. El-Mazry, C.; Correc, O.; Colin, X. *Polym. Degrad. Stab.* **2012**, *97*, 1049.
11. Flory, P. J. Principles of Polymer Chemistry; Cornell University Press: Ithaca, **1953**.
12. Fermeglia, M.; Pricl, S. *Prog. Org. Coat.* **2007**, *58*, 187.
13. Kremer, K.; Müller-Plathe, F. *Mol. Simul.* **2002**, *28*, 729.
14. Bouvard, J. L.; Ward, D. K. *J. Eng. Mater. Technol.* **2009**, *131*, 041206.
15. van Krevelen, D. W. Properties of Polymers; Elsevier: Amsterdam, **1990**.
16. Halpin, J. C.; Kardos, J. L. *J. Appl. Phys.* **1972**, *43*, 2235.
17. Sakurada, I.; Kaji, K. *J. Polym. Sci. Part C: Polym. Lett.* **1970**, *31*, 57.
18. Flory, P. J.; Williams, A. D. *J. Polym. Sci. Part A-2: Polym. Phys.* **1967**, *5*, 399.
19. Silva, L.; Tognana, S.; Salgueiro, W. *Polym. Test.* **2013**, *32*, 158.
20. Seitz, J. T. *J. Appl. Polym. Sci.* **1993**, *49*, 1331.
21. Fox, T. G.; Loshaek, S. *J. Polym. Sci.* **1955**, *15*, 371.
22. Lennard-Jones, J. E. *Proc. R. Soc. Lond.* **1924**, *106*, 463.
23. Wu, S. *Polym. Eng. Sci.* **1990**, *30*, 753.
24. Kausch, H. H.; Heymans, N.; Plummer, C. J.; Decroly, P. Matériaux polymères: propriétés mécaniques et physiques; Presses Polytechniques et Universitaires Romandes: Lausanne, **2001**.
25. Domingos, E.; Pereira, T. M. C.; Filgueiras, P. R.; Bueno, M. I. M. S.; de Castro, E. V. R.; Guimarães, R. C. L.; de Sena, G. L.; Rocha, W. F. C.; Romão, W. *X-Ray Spectrom.* **2013**, *42*, 79.
26. Karacan, I. *Fibers Polym.* **2005**, *6*, 186.